Journal of Coordination Chemistry

ISSN: 0095-8972 (Print) 1029-0389 (Online) Journal homepage: http://www.tandfonline.com/loi/gcoo20

Synthesis, structure, and thermal decomposition of two copper coordination compounds $[Cu(DAT)_2(PA)_2]$ and $[Cu(DAT)_2(HTNR)_2]$ with nitrogen rich 1,5-diaminotetrazole (DAT)

Yan-Gang Bi, Yong-An Feng, Ying Li, Bi-Dong Wu & Tong-Lai Zhang

To cite this article: Yan-Gang Bi, Yong-An Feng, Ying Li, Bi-Dong Wu & Tong-Lai Zhang (2015) Synthesis, structure, and thermal decomposition of two copper coordination compounds $[Cu(DAT)_2(PA)_2]$ and $[Cu(DAT)_2(HTNR)_2]$ with nitrogen rich 1,5-diaminotetrazole (DAT), Journal of Coordination Chemistry, 68:1, 181-194, DOI: 10.1080/00958972.2014.981167

To link to this article: http://dx.doi.org/10.1080/00958972.2014.981167

Accepted author version posted online: 28 Oct 2014.
Published online: 17 Nov 2014.

Journal of Coordination Chemistry, 2015
Vol. 68, No. 1, 181–194, http://dx.doi.org/10.1080/00958972.2014.981167

Synthesis, structure, and thermal decomposition of two copper coordination compounds $[Cu(DAT)_2(PA)_2]$ and $[Cu(DAT)_2(HTNR)_2]$ with nitrogen rich 1,5-diaminotetrazole (DAT)

YAN-GANG BI, YONG-AN FENG, YING LI, BI-DONG WU and TONG-LAI ZHANG*

State Key Laboratory of Explosion Science and Technology, Beijing Institute of Technology, Beijing, PR China

(*Received 30 April 2014; accepted 2 October 2014*)

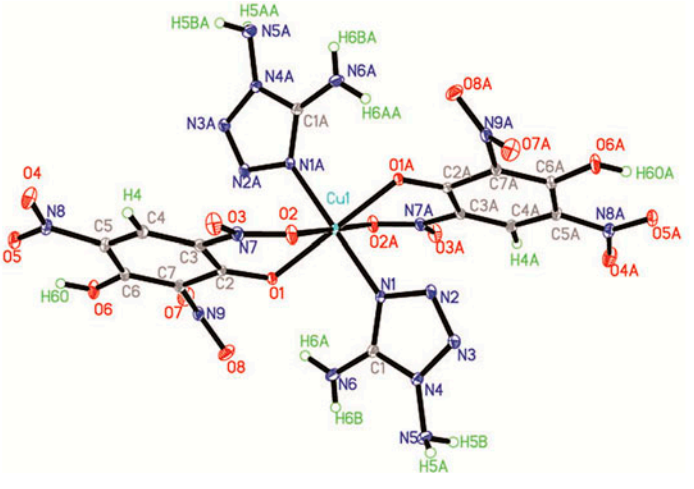

Two similar complexes combined with 1,5-diaminotetrazole (DAT) and copper trinitrophenol were characterized by elemental analysis, FT-IR spectroscopy and single crystal X-ray diffraction and the sensitivity were studied.

Both $[Cu(DAT)_2(PA)_2]$ (**1**) and $[Cu(DAT)_2(HTNR)_2]$ (**2**) were prepared from 1,5-diaminotetrazole (DAT) and copper trinitrophenol, **1** for picrate (PA) and **2** for styphnate acid (2,4,6-trinitro resorcinol, TNR), and were characterized by elemental analysis, FT-IR spectroscopy, and single crystal X-ray diffraction. The space group of these compounds is $P2_1/c$ (monoclinic). The lattice parameters are similar [$a = 11.405(3)$ Å, $b = 14.867(3)$ Å, $c = 8.099(2)$ Å for **1** and $a = 12.262(3)$ Å, $b = 14.900(3)$ Å, $c = 7.243(2)$ Å for **2**], except the $\beta = 106.257(3)°$ in **1** and $\beta = 92.989(4)°$ in **2**. Both have extended structures due to hydrogen bonds, but there are some differences because of the ligands induced effect. Differential scanning calorimetry analysis shows that two exothermic processes take place in both complexes, the first peak temperatures are 488.2 K for **1** and 519.2 K

*Corresponding author. Email: ztlbit@bit.edu.cn

for **2**. The kinetic parameters of the first exothermic process were studied by using Kissinger's method and Ozawa's method, in which the enthalpy of formation (−7346 and −5706 kJ M^{-1}), critical temperature of thermal explosion (475.0 and 515.8 K), entropy of activation ($\Delta S^{\neq}$), enthalpy of activation ($\Delta H^{\neq}$), and free energy of activation ($\Delta G^{\neq}$) were calculated and obtained as −117.25 J K^{-1} M^{-1}, 140.64 kJ M^{-1}, 196.44 kJ M^{-1} and −219.1 J K^{-1} M^{-1}, 383.56 kJ M^{-1}, 495.34 kJ M^{-1} for **1** and **2**, respectively. The sensitivity test results showed that both compounds were sensitive to impact (<5 J) and flame (>20 cm) rather than friction.

Keywords: 1,5-Diaminotetrazole; Picrate and styphnate; Copper; Kinetic parameters; Sensitivity

Introduction

Since nitrogen heterocycles offer higher heat of formation, larger density, and better oxygen balance than their carbocyclic analogs, these kinds of compounds have attracted interest in synthesis of high energy density materials [1–3]. Aminotetrazoles have high nitrogen content, large positive enthalpies, and high thermal stabilities [4–6]. They play roles as ligands to form energetic complexes [7–15] or as anions to construct energetic salts together with guanidine, amine, etc. [16–22].

1,5-Diaminotetrazole (DAT) is one of the highest nitrogen content (84.0 wt%) compounds and is shown in figure 1. N1 is fully occupied by $-NH_2$, N2, and C, while the other five nitrogens remain to participate in coordination, especially at the 4th-position [23–25].

In our recent research, we found that picric acid (2,4,6-trinitrophenol, PA) and styphnate acid (2,4,6-trinitro resorcinol, TNR) can form energetic salts and coordination compounds as outer anions [26]. However, in most cases, complexes which are based on PA and TNR contain either coordination waters and/or lattice waters, such as $[Co(DAT)_6](PA)_2{\cdot}4H_2O$, $[Zn(DAT)_2(H_2O)_4](PA)_2{\cdot}2H_2O$, and $[Co(DAT)_2(H_2O)_4](HTNR)_2{\cdot}2H_2O$ [27–29].

In this article, two crystal structures, $[Cu(DAT)_2(PA)_2]$ (**1**) and $[Cu(DAT)_2(HTNR)_2]$ (**2**), were synthesized and determined by FT-IR analyses. Furthermore, the thermal decomposition mechanism for **1** and **2** was predicted based on DSC and TG-DTG. The non-kinetic parameters of the first exothermic process were determined by applying the Kissinger method and Ozawa method. In addition, we found that **2** was more sensitive than **1** in flame and impact sensitivity.

Experimental

General caution

The title compounds are energetic materials and tend to explode under certain conditions. Appropriate safety precautions (safety glasses, face shields, leather coat, and ear plugs) should be taken, especially when the compound is prepared on a large scale and in dry state.

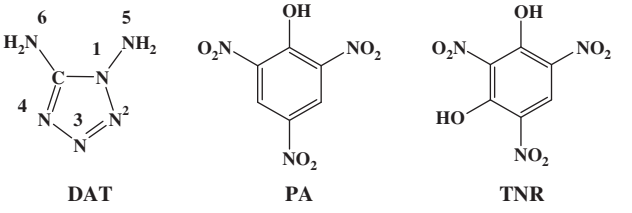

Figure 1. The structure of 1,5-diaminotetrazole (CN_6H_4, DAT), PA and TNR.

Materials and physical technique

All the reagents and solvents were of analytical grade and used as commercially obtained. Elemental analyses were performed on a Flash EA 1112 full-automatic trace element analyzer. The FT-IR spectra were recorded on a Bruker Equinox 55 infrared spectrometer (KBr pellets) from 4000 to 400 cm^{-1} with a resolution of 4 cm^{-1}. DSC and TG measurements were carried out with a Pyris-1 differential scanning calorimeter and Pyris-1 thermogravimetric analyzer (PerkinElmer, USA) under dry nitrogen with flow rate of 20 mL min^{-1}. The combustion heat was measured by oxygen bomb calorimeter (Parr 6200, USA).

Synthesis of 1. DAT (0.51 g, 5 mM) and PA (0.45 g, 2 mM) were dissolved in 30 mL H_2O and stirred for half an hour at 343.2 K. Then, $CuCl_2$ (0.34 g, 2 mM) in the same solvent was added gradually dropwise under stirring. The suspension was stirred for another hour and filtered immediately into a cup. After one day, green crystals suitable for X-ray analysis were obtained in 75% yield. Elemental analysis for $C_{14}H_{12}CuN_{18}O_{14}$: C, 23.36; N, 35.02; H, 1.68. Found: C, 23.27; N, 34.95; H, 1.73. IR (KBr) ν: 3411, 3308, 1671, 1634, 1561, 1486, 1437, 1369, 1335, 1272, 1158, 1079, 935, 906, 742, 704, 519 cm^{-1}.

Synthesis of 2. The synthesis progress of **2** is similar with **1**, only using TNR instead of PA in 80 mL H_2O; after a few hours, green crystals are obtained in 60% yield. Elemental analysis for $C_{14}H_{12}CuN_{18}O_{14}$: C, 22.36; N, 33.53; H, 1.61. Found: C, 22.41; N, 33.46; H, 1.65. IR (KBr) ν: 3448, 3335, 2294, 1682, 1623, 1573, 1534, 1323, 1195, 1129, 1090, 1015, 924, 787, 698 cm^{-1}.

X-ray data collection and structure refinement

The X-ray diffraction data collection was performed on a Rigaku AFC-10/Saturn 724^+ CCD detector diffractometer with graphite-monochromated Mo K_α radiation (λ = 0.71073 Å) with φ and ω modes at 153(2) K. The structure was solved by direct methods using SHELXS–97 [30] and refined by full-matrix least-squares methods on F^2 with SHELXL–97 and Olex-2 [31]. Detailed information concerning crystallographic data collection and structure refinement are summarized in table 1.

Results and discussion

Synthesis

Compound **1** was synthesized and collected in aqueous solution with pH 1, and thus, we inferred that a similar compound **2** would be got by the reaction of DAT and $CuCl_2$ with HTNR in the same condition. However, precipitation was formed when $CuCl_2$ was added into the mixed solution of DAT and HTNR; although the pH 1 was the same, few crystals

Table 1. Crystallographic data and structure refinements for **1** and **2**.

Compound	$Cu(DAT)_2(PA)_2$	$Cu(DAT)_2(HTNR)_2$
CCDC	969660	988711
Empirical formula	$CuC_{14}H_{12}N_{18}O_{14}$	$CuC_{14}H_{12}N_{18}O_{16}$
Formula mass /g M^{-1}	719.96	751.96
Crystal system	Monoclinic	Monoclinic
Space group	$P2_1/c$	$P2_1/c$
Crystal dimension /mm	0.55 × 0.36 × 0.25	0.52 × 0.37 × 0.13
Z	2	2
a, b, c /Å	11.405(3), 14.867(3), 8.099(2)	12.262(3), 14.900(3), 7.2431(17)
β /°	106.257(3)	92.989(4)
h, k, l	$-14 \le h \le 15, -20 \le k \le 20, -11 \le l \le 10$	$-16 \le h \le 15, -20 \le k \le 19, -9 \le l \le 9$
V /Å^3	1318.3(4)	1321.6(5)
D_c /(g cm^{-3})	1.81	1.89
μ (Mo K_α) /mm^{-1}	0.154	0.941
F(0 0 0)	726	758
θ Range /°	2.31–29.13	5.46–58
Measured reflections	13,494	11,058
Unique data	3534 [$R_{int} = 0.034$]	3504 [$R_{int} = 0.0364$]
R_1, wR_2 [$I > 2\sigma(I)$]	0.0398, 0.0944	0.0389, 0.0989
R_1, wR_2 (all data)	0.0464, 0.0990	0.0442, 0.1032
Goodness of fit	0.998	1.001
δp_{max}, δp_{min} /(eÅ^{-3})	0.45, −0.44	0.42, −0.51

Note: (a) $wR_2 = [\sum w(F_o^2 - F_c^2)^2 / \sum w(F_o^2)]^{1/2}$, $P = (F_o^2 + 2F_c^2)/3$. (b) $w = 1/[\sigma^2(F_o^2) + (0.0510P)^2 + 0.1600P]$.

were collected. After an extended series of experiments over a long period, we concluded that the key drivers in that expected increase in yield of **2** will be increased amount of H_2O. Thus, the use of H_2O in the synthesis of **2** was 80 mL instead of 30 mL for **1** to get the best yield.

Molecular structure of 1 and 2

Compound **1** as well as **2** crystallizes in monoclinic and space group $P2_1/c$ (figure 2). The octahedral copper ion at the inversion center is equatorially coordinated by two nitrogens from two DAT molecules and four oxygens from two PA anions for **1** and HTNR anions for **2**, respectively. There are neither coordinated nor lattice waters. The two DAT molecules

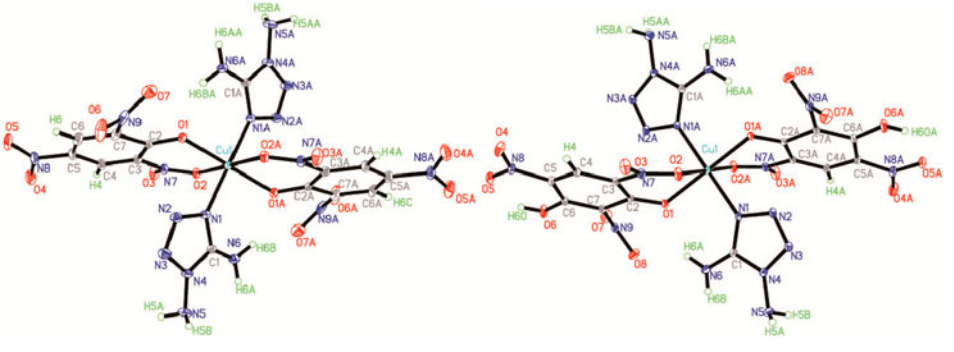

Figure 2. The molecular structures of **1** (left) and **2** (right).

are coordinated with copper at the 4th position in both compounds. The benzene rings of either PA or HTNR anions are parallel. The lattice parameters of **1** are as follows: $a = 11.405(3)$ Å, $b = 14.867(3)$ Å, $c = 8.099(2)$ Å, and $\beta = 106.257(3)°$, however, in **2**: $a = 12.262(3)$ Å, $b = 14.900(3)$ Å, $c = 7.243(2)$ Å are similar to **1**, only the $\beta = 92.989(4)°$ is closer than that in **1**.

The geometric parameters around Cu^{2+} in **1** are Cu1–N1 = 1.984(2) Å, Cu1–O1 = 1.933 (2) Å, Cu1–O2 = 2.339(2) Å, while in **2,** the bond lengths Cu1–N1 = 2.0029(15) Å, Cu1–O1 = 1.9651(12) Å, Cu1–O2 = 2.3625(15) Å are longer than those in **1** because of the existence of the other hydroxyl group of HTNR ion. The selected bond lengths and angles are listed in table 2. In addition, the density of **2**, 1.89 g cm^{-3}, is larger than that in **1** (1.81 g cm^{-3}).

There are twelve hydrogens in both complexes**,** but a few inner molecular hydrogen bonds in them. For **1**, the only two inner molecular hydrogen bonds are N6–H6A···O7 = 2.396(6) Å and N6–H6A···O1 = 2.087(9) Å. In **2**, the inner molecular hydrogen bonds are O6–H6O···O5 = 1.90(3) Å, N6–H6A···O1 = 2.09(3) Å, and N6–H6A···O8 = 2.37(2) Å. All of the hydrogen bonds in both **1** and **2** are calculated by Platon and listed in table 3.

The two title complexes form a 3-D network because of the hydrogen bonds, and their packing views along the *c*-axis are shown in figures 3 and 4, respectively.

As shown in figure 1, the two different DAT rings of **1** are coplanar (angle = 0.00(66)), while two benzene rings of PA anions are in two parallel surfaces. If they are approximately for the same plane, two kinds of intersecting planes are shown in figure 3, which is the packing view of **1** along the *c*-axis, on the left is the typical amplification part of the right in order to see more clearly the hydrogen bond. The projection of DAT rings is overlapped and forms parallel straight lines, along which intersecting planes of PA rings appear alternately. Furthermore, they are inclined to one another at an angle of 56.317.

Table 2. Selected bond lengths and angles for **1** and **2**.

Compound **1**			
Atoms 1,2	Lengths /Å	Atoms 1,2	Lengths/Å
Cu1–O1	1.9333(14)	Cu1–$O2^i$	2.3398(14)
Cu1–$O1^i$	1.9333(14)	Cu1–O2	2.3398(14)
Cu1–$N1^i$	1.9845(16)	Cu1–N1	1.9846(16)
Atoms 1,2,3	Angles /°	Atoms 1,2,3	Angles /°
$N1^i$–Cu1–$O2^i$	87.94(6)	N1–Cu1–O2	87.94(6)
O1–Cu1–$N1^i$	88.95(6)	N1–Cu1–$O2^i$	92.06(6)
$O1^i$–Cu1–$N1^i$	91.05(6)	O1–Cu1–O2	79.38(5)
O1–Cu1–N1	91.05(6)	O1–Cu1–$O2^i$	100.62(5)
$O1^i$–Cu1–N1	88.95(6)	$O1^i$–Cu1–$O2^i$	79.38(5)
Compound **2**			
Atoms 1,2	Lengths /Å	Atoms 1,2	Lengths /Å
Cu1–O1	1.9651(12)	Cu1–$O2^i$	2.3625(15)
Cu1–$O1^i$	1.9651(12)	Cu1–O2	2.3625(15)
Cu1–$N1^i$	2.0029(15)	Cu1–N1	2.0029(15)
Atoms 1,2,3	Angles /°	Atoms 1,2,3	Angles /°
$N1^i$–Cu1–$O2^i$	88.29(6)	N1–Cu1–O2	88.29(6)
O1–Cu1–$N1^i$	88.49(6)	N1–Cu1–$O2^i$	91.71(6)
$O1^i$–Cu1–$N1^i$	88.49(6)	O1–Cu1–O2	77.90(5)
O1–Cu1–N1	91.51(6)	O1–Cu1–$O2^i$	102.10(5)
$O1^i$–Cu1–N1	91.51(6)	$O1^i$–Cu1–$O2^i$	77.90(5)

Note: (i) $1 - x$, $1 - y$, $1 - z$.

Table 3. Selected hydrogen bonds and angles for **1** and **2**.

Compound **1**				
D–H···A	*d*(D–H)	*d*(H···A)	*d*(D···A)	*a*(D–H···A)
N5–H5A···O2#1	0.880(0)	2.588(2)	3.146(2)	122.1(2)
N5–H5B···O2#2	0.840(0)	2.41(3)	2.946(3)	122(2)
N6–H6B···N5	0.880(9)	2.518(9)	2.878(2)	105.3(8)
N6–H6B···O5#3	0.880(9)	2.289(9)	3.079(2)	149.3(8)
N6–H6A···O1#4	0.880(10)	2.087(9)	2.817(2)	139.8(9)
N6–H6A···O7#4	0.880(10)	2.396(9)	3.069(3)	133.6(6)
C4–H4···O6#5	0.950(2)	2.450(2)	3.305(2)	149.57(19)
Compound **2**				
D–H···A	*d*(D–H)	*d*(H···A)	*d*(D···A)	*a*(D–H···A)
N5–H5A···O5#i	0.86(3)	2.35(3)	3.136(3)	152(2)
N5–H5A···N3#ii	0.86(3)	2.59(3)	3.077(3)	117(2)
N5–H5B···O7#iii	0.82(3)	2.37(3)	3.048(3)	141(3)
N6–H6A···O1	0.85(3)	2.09(3)	2.789(2)	139(3)
N6–H6A···O8	0.85(3)	2.37(2)	3.111(2)	145(3)
N6–H6B···O2#iv	0.81(3)	2.40(3)	3.039(3)	136(2)
N6– H6B···N5	0.81(3)	2.57(2)	2.878(3)	105(2)
O6–H6O···O5	0.85(3)	1.90(3)	2.613(2)	141(3)
O6–H6O···N3#v	0.85(3)	2.34(4)	2.985(2)	133(3)
O6–H6O···N8	0.85(3)	2.50(3)	2.938(2)	113(3)

Note: Symmetry transformations for **1**: #1 $1-x,1/2+y,1/2-z$; #2 $x,3/2-y,1/2+z$; #3 $-1+x,3/2-y,-1/2+z$; #4 $1-x,1-y,1-z$; #5 $x,y,-1+z$. Symmetry transformations for **2**: #i $1+x,3/2-y,1/2+z$; #ii $x,3/2-y,1/2+z$; #iii $1-x,1-y,2-z$; #iv $x,y,1+z$; #v $-1+x,y,z$.

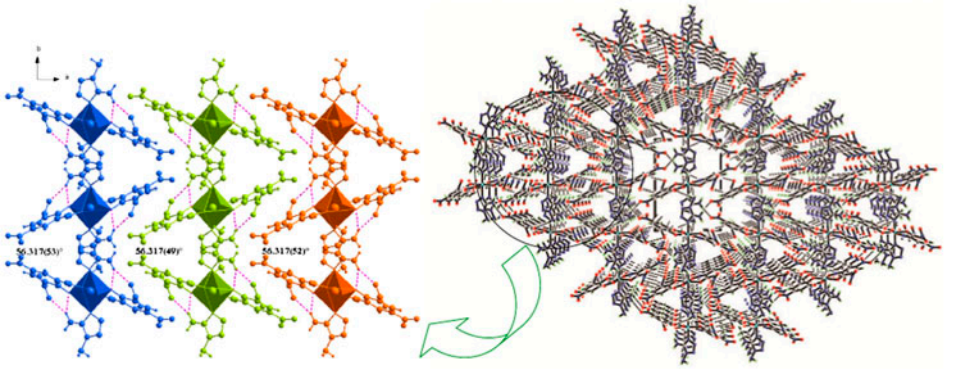

Figure 3. Packing view of **1** along the *c*-axis.

Figure 4, which is much different compared to figure 3, is the packing view of **2** along the *c*-axis, and the right part is for clarity. First, the plane of DAT rings intersects instead of forming lines. Second, the two benzene rings from HTNR ligand cannot be approximately the same plane, but like "pliers", however, the $-NO_2$ and $-NH_2$ surround the "pivots" of the "pliers" in the packing view. Third, the two benzene rings, from adjacent molecules, are close to each other parallel on the *b*-axis. These differences arise from the different ligand, inducing another orientation of Cu polyhedron within the unit cell due to ligand size variations and differences in intermolecular interactions compared with **1**.

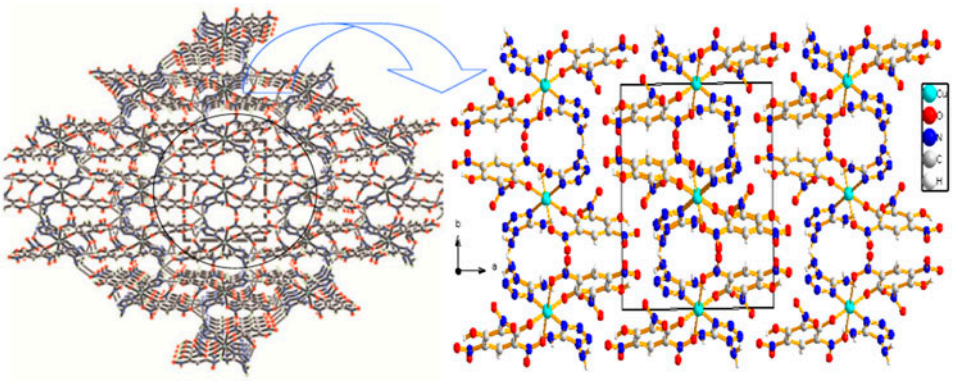

Figure 4. Packing view of **2** along the *c*-axis.

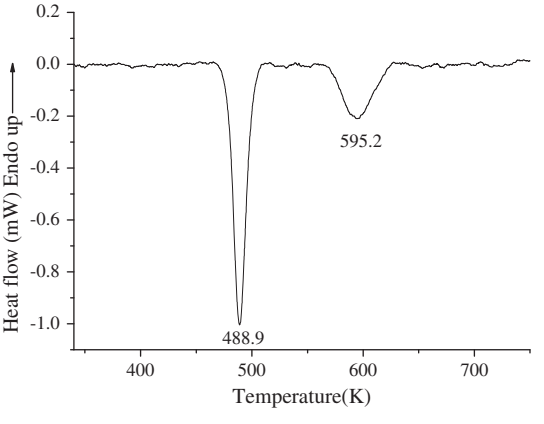

Figure 5. The DSC curve for **1** in a nitrogen atmosphere with heating rate of 10 K min^{-1}.

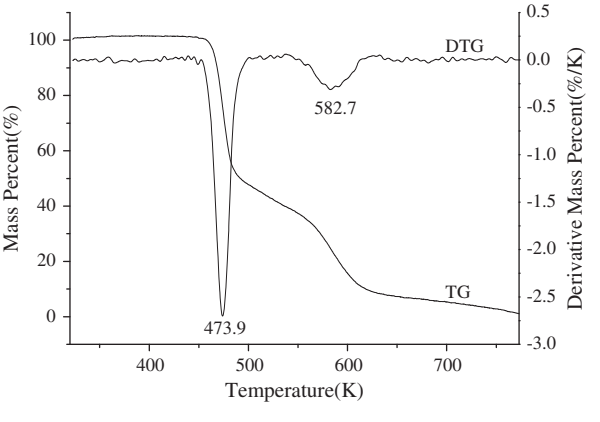

Figure 6. The TG-DTG curves for **1** in a nitrogen atmosphere with heating rate of 10 K min^{-1}.

However, there are similarities in both compounds, the central copper ions can be transformed into each other by translation along the *a*-axis, while they are symmetrical with each other on the *b*-axis.

Thermal decomposition

With the purpose of investigating the thermal behavior of **1** and **2**, DSC and DTG curves with the linear heating rate of 10 K min^{-1} were recorded in a nitrogen atmosphere (figures 5 and 6 for **1** and figures 7 and 8 for **2**).

There are two exothermic processes on the DSC curve for **1**; the peak temperatures are 488.9 and 595.2 K. Correspondingly, there are two main mass loss stages in the TG-DTG curves. The first stage occurs from 463.2 to 523.2 K with a mass loss of 57%, in which the largest mass loss rate is reached at 473.2 K with a mass loss percentage of 2.9% K^{-1}. This process shows the main exothermic decomposition of the ligands and picrate anions. Then,

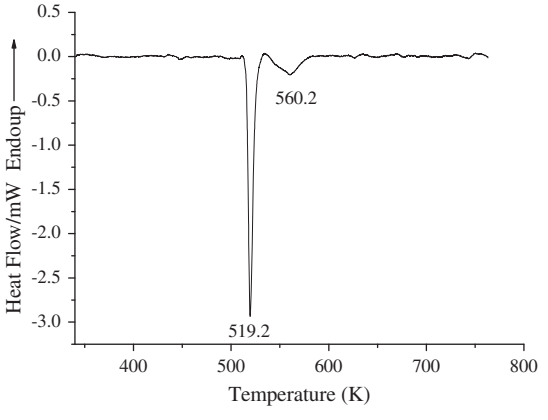

Figure 7. The DSC curve for **2** in a nitrogen atmosphere with heating rate of 10 K min^{-1}.

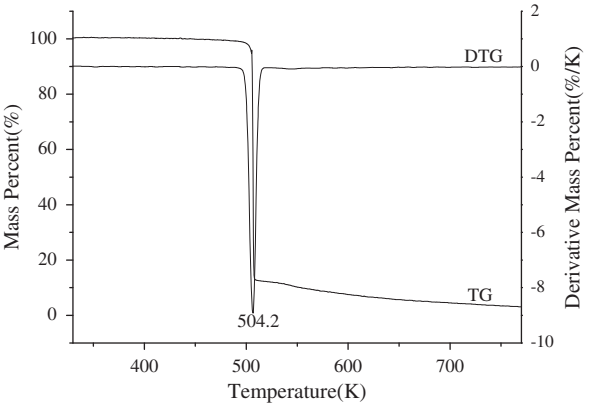

Figure 8. The TG-DTG curves for **2** in a nitrogen atmosphere with heating rate of 10 K min^{-1}.

one mass loss appeared from 523.2 to 623.2 K with mass loss of 33%. It is the secondary decomposition process of the decomposed residues from the first stage.

There are also two exothermic processes on the DSC curve for **2**, but the first peak temperature is 519.2 K and is higher than that of **1**. The second peak temperature is 560.2 K and is lower than 595.2 K on the DSC curve of **1**. Correspondingly, there are two main mass loss stages in the TG-DTG curves as well. The first stage occurs from 447.2 to 517.2 K with a mass loss of 87.66%, in which the largest mass loss rate reached at 504.2 K with a mass loss percentage of 62.8% K^{-1}, and there is a sharp weight loss on the coordinated TG curves. This process shows the main exothermic decomposition of the ligands and styphnate anions. One successive mass loss stage appeared from 523.2 to 587.2 K with mass loss of 4.2%, as a secondary decomposition process and the decomposition rate slower than that in the first stage.

Energies of combustion and enthalpies of formation

In order to study the energy of combustion and the enthalpy of formation of **1** and **2**, the constant volume energy of combustion (Q_v) was measured by oxygen bomb calorimetry and was determined to have a value of −10,160 kJ kg^{-1} for **1**, while the combustion energy of **2** is lower, only −7548.3 kJ kg^{-1}. According to the bomb combustion, reaction equations as follows:

$$CuC_{14}N_{18}O_{14}H_{12}(s) + 21/2O_2(g) = CuO(s) + 14CO_2(g) + 9N_2(g) + 6H_2O(l) \quad (1)$$

$$CuC_{14}N_{18}O_{16}H_{12}(s) + 19/2O_2(g) = CuO(s) + 14CO_2(g) + 9N_2(g) + 6H_2O(l) \quad (2)$$

The energy of combustion can be ($T = 298.15$ K) as follows:

$$\Delta H_1 = Q_{P1} = Q_{V1} + \Delta n_1 RT = -7346\text{kJ M}^{-1} = -10,200 \text{ kJ kg}^{-1} \quad (3)$$

$$\Delta H_2 = Q_{P2} = Q_{V2} + \Delta n_2 RT = -5706\text{kJM}^{-1} = -7588 \text{ kJ kg}^{-1} \quad (4)$$

Thus, the energy of combustions is −10,200 kJ kg^{-1} for **1** and −7588 kJ kg^{-1} for **2**.

In accordance with the known enthalpies of formation of [$\Delta_f H°_{298}$(CuO(s)) = −155.2 kJ·M^{-1}], carbon dioxide [$\Delta_f H°_{298}(CO_2(g)) = -393.5$ kJ M^{-1}], and water [$\Delta_f H°_{298}(H_2O(l)) = -285.8$ kJ M^{-1}] [32], the standard enthalpies of formation were back calculated from the energies of combustion on the basis of equations 1 and 2, and Hess's Law as applied in thermochemical equations (3) and (4). The enthalpies of formation of **1** and **2** are as follows:

$$\begin{aligned}\Delta_f H^\circ_{298}(\mathbf{1}, s) &= \Delta_f H^\circ(\text{CuO,s}) + 6\Delta_f H^\circ(H_2O, 1) + 14\Delta_f H^\circ(CO_2, g) - \Delta_c H^\circ(\mathbf{1}, s) \\ &= -37.5\text{kJ mol}^{-1}\end{aligned} \quad (5)$$

$$\Delta_f H^{\circ}_{298}(\mathbf{2}, s) = \Delta_f H^{\circ}(CuO,s) + 6\Delta_f H^{\circ}(H_2O, 1) + 14\Delta_f H^{\circ}(CO_2, g) - \Delta_c H^{\circ}(\mathbf{2}, s) = -1673 \text{kJ mol}^{-1} \quad (6)$$

Non-isothermal kinetics analysis

Kissinger's and Ozawa's methods are widely used to determine the Arrhenius equation for a given material. The Kissinger equation (7) [33] and Ozawa equation (8) [34] are as follows:

$$\ln \beta/T_p^2 = \ln [RA/E_a] - E_a/(RT_p) \quad (7)$$

$$\lg \beta = \lg[AE_a/RG(\alpha)] - 2.315 - 0.4567E_a/RT_p \quad (8)$$

T_p is the peak temperature at which the exothermic peak occurs in the DSC curve (K), A is the pre-exponential factor (s^{-1}), E_a is the apparent activation energy (kJ M^{-1}), R is the gas constant (8.314 J K^{-1} M^{-1}), β is the linear heating rate (K min^{-1}), and G (α) is the reaction–mechanism function.

While there were many ways to calculate the kinetics parameters, Kissinger and Ozawa's methods were established on the basis of the temperatures at which the first exothermic peaks occur in the DSC curves measured with four different heating rates (5, 10, 15, and 20 K min^{-1}) of **1** and **2**. From these data, the apparent activation energy E_k and E_o, pre-exponential factor A_k, and linear coefficient R_k and R_o were determined and listed in table 4. Accordingly, the Arrhenius equations of **1** and **2** can be expressed as follows (E is the average of E_k and E_o):

$$\ln k = 13.52 - 144.6 \times 10^3/(RT) \text{ for} \mathbf{1} \quad (9)$$

Table 4. The peak temperatures of the exothermal peaks at different heating rates and the kinetic parameters.

Heating rates (K min^{-1})	$Cu(DAT)_2PA_2$ Peak temperatures T_p /K	$Cu(DAT)_2(HTNR)_2$ Peak temperatures T_p /K
5	479.2	515.6
10	488.9	519.6
15	493.9	522.1
20	497.0	523.1
Kissinger's method		
E_k /(kJ M^{-1})	144.3	393.3
ln$A$	13.52	38.02
Linear correlation coefficient R_k	−0.9979	−0.9969
Standard deviation	0.0456	0.0572
Ozawa's method		
E_o /(kJ M^{-1})	144.9	382.2
Linear correlation coefficient R_o	−0.9981	−0.997
Standard deviation	0.0199	0.0248

$$\ln k = 38.02 - -387.8 \times 10^3/(RT) \text{ for} \mathbf{2} \tag{10}$$

Calculation of critical temperature of thermal explosion, $\Delta S^{\neq}$, $\Delta H^{\neq}$, and $\Delta G^{\neq}$

The values of the peak temperatures corresponding to $\beta \rightarrow 0$ obtained according to equation (11) [35], where a, b, and c are coefficients. T_{p0} value is calculated at 462 K and 510 K for **1** and **2**, respectively.

$$T_{pi} = T_{p0} + a\beta + b\beta^2 + c\beta^3 + d\beta^4 \tag{11}$$

The corresponding critical temperatures of thermal explosion (T_b) obtained were 475 K for **1** and 515.8 K for **2** by equation (12) [35]. E is in accord with equations (9) and (10).

$$T_b = \frac{E - \sqrt{E^2 - 4ERT_{p0}}}{2R} \tag{12}$$

The entropies of activation ($\Delta S^{\neq}$), enthalpies of activation ($\Delta H^{\neq}$), and free energies of activation ($\Delta G^{\neq}$) of the decomposition reaction of **1** corresponding to $T = T_{p0}$ and $A = A_k$ (Kissinger's method) obtained by equations (13–15) [35] were -226.9 J K^{-1}M^{-1}, 140.76 kJ M^{-1}, 245.58 kJ M^{-1} for **1** and -219.1 J K^{-1}M^{-1}, 383.56 kJ M^{-1}, 495.34 kJ M^{-1} for **2**,

$$A = \frac{k_B T}{h} e^{\Delta S^{\neq}/R} \tag{13}$$

$$\Delta H^{\neq} = E - RT \tag{14}$$

$$\Delta G^{\neq} = \Delta H^{\neq} - T\Delta S^{\neq} \tag{15}$$

where k_B is the Boltzmann constant/1.381×10^{-23} (J K^{-1}) and h is the Planck constant/6.626×10^{-34} (J s).

Sensitivity tests

The impact and friction sensitivities as well as the flame sensitivity were determined based on the China National Military Standard as shown in table 5.

Impact sensitivity was determined by a fall hammer apparatus. Salt (30 mg) was placed between two steel poles and was hit by 5.0 kg drop hammer. The test results showed that the firing height for **1** and **2** is 8.5 and 3 cm, respectively.

Friction sensitivity was determined on a MGY-1 pendular friction sensitivity apparatus by a standard procedure using 20 mg of sample. When salt was compressed between two steel poles with mirror surfaces at pressure of 3.92 MPa and then was hit horizontally with a 1.5 kg hammer from 90° angle, the firing rates were 0% for **1** and **2**.

Table 5. Physicochemical properties of **1** and **2**.

	$Cu(DAT)_2(PA)_2$ (**1**)	$Cu(DAT)_2(HTNR)_2$ (**2**)
Formula	$CuC_{14}H_{12}N_{18}O_{14}$	$CuC_{14}H_{12}N_{18}O_{16}$
Mol. mass [g M^{-1}]	719.96	751.96
D_c [g cm^{-3}]	1.81	1.89
T_{p0} [K][a]	462	510
T_b [K][b]	475.2	515.8
$\Delta H^{\neq}$ [kJ M^{-1}][c]	140.76	383.56
$\Delta S^{\neq}$ [J K^{-1} M^{-1}][d]	−226.9	−219.1
$\Delta G^{\neq}$ [kJ M^{-1}][e]	245.58	495.34
T_d [K][f]	488.9	519.6
N [%][g]	35	33.5
N + O [%][h]	66.1	67.6
Ω [%][i]	−44.5	−38.3
E [kJ M^{-1}]	144.6	387.8
Q_v [kJ kg^{-1}]	−10,160	−7548.3
$\Delta H = Q_P$ [kJ kg^{-1}]	−10,200	−7588
$\Delta_f H°_{298}$ [kJ M^{-1}]	−37.5	−1673
Impact sensitivity [J]	4.25	1.5
Friction sensitivity [%]	–	–
Flame sensitivity h_{50} [cm]	23	25

[a]The values of the peak temperatures corresponding to $\beta \rightarrow 0$.
[b]The corresponding critical temperatures of thermal explosion.
[c]Enthalpies of activation.
[d]Entropies of activation.
[e]Free energies of activation [30].
[f]Thermal degradation /DSC main exothermic peak.
[g]nitrogen content.
[h]nitrogen and oxygen content.
[i]oxygen balances.

Flame sensitivity was determined by a standard method, in which the sample was ignited by standard black powder pellet. Salt (20 mg) was compacted to a copper cap under the press of 58.8 MPa and was ignited by standard black powder pellet. The test results showed that the 50% firing heights (h_{50}) were 23 cm for **1** and 25 cm for **2**.

Thus, we found that both **1** and **2** have high impact and flame sensitivity, but low friction sensitivity.

Physicochemical properties

The mentioned physicochemical properties of **1** and **2** are listed in table 5. Their oxygen balances are better than TNT ($\Omega = -74\%$). More importantly, the nitrogen contents of both compounds are more than 30%, the nitrogen and oxygen contents are no less than 66%. Compared with the known combustion energies of RDX (1,3,5-trinitro-1,3,5-triazacyclohexane), HMX (1,3,5,7-tetranitro-1,3,5,7-tetraazocane), and TNT (2,4,6-trinitrotoluene), which were reported as −9600, −9880 and −15,220 kJ kg^{-1}, respectively [35], the combustion value of **1** was higher than that of RDX and HMX, but lower than that of TNT. The order of combustion values for these energetic compounds is **2** < RDX < HMX < **1** < TNT.

Lower values of T_b, 475.2 K for **1** and 515.8 K for **2**, show that the transition from thermal decomposition to thermal explosion is easy to take place, especially for **1**. We found that the yields increased when reaction temperature is elevated for both compounds in accord with the positive values of $\Delta G^{\neq}$. In light of the sensitivity, both compounds are more sensitive to impact and flame than friction.

Conclusion

$[Cu(DAT)_2(PA)_2]$ and $[Cu(DAT)_2(HTNR)_2]$ were synthesized, and the crystal structures were studied. There were no crystal waters in **1** and **2**; PA and HTNR are able to coordinate with the metal ion through the oxygens from –OH and $–NO_2$ instead of as an outer anion. The DSC curve shows two exothermic processes from 463.2 to 623.2 K for **1** and from 447.2 to 587.2 K for **2** corresponding to TG-DTG curves, but their decomposition temperature are lower than $[Ca(tza)_2(H_2O)_2]_n$ 555.2 K [36].

The results of the non-isothermal kinetic analysis indicated that the Arrhenius equation of **1** and **2** can be expressed as $\ln k = 13.52 - 144.6 \times 10^3/(RT)$ (**1**) and $\ln k = 38.02 - 387.8 \times 10^3/(RT)$ (**2**). The order of combustion for these energetic compounds is **2** < RDX < HMX < **1** < TNT. The sensitivity properties indicated that both compounds had lower friction, but high impact sensitivity and flame sensitivity.

As observed with Cu(HATZ)(PDA)(H_2O) (HATZ = 5-aminotetrazole, H_2PDA = pyridine-2,6-dicarboxylic acid) [37], $[Cd(IMI)_2(N_3)_2]_n$ (IMI = imidazole) [38], $[Ca(tza)_2(H_2O)_2]_n$ (tza = tetrazole acetic acid) [36], and zinc-FOX-7 complex (FOX-7 = 1,1-diamino-2,2-dinitroethylene) [39], both of the title compounds show higher sensitivity.

Supplementary material

Crystallographic data (excluding structure factors) for the structures in this article have been deposited with the Cambridge Crystallographic Data Center, CCDC, 12 Union Road, Cambridge CB21EZ, UK. Copies of the data can be obtained free of charge on quoting the depository numbers CCDC-969660 and CCDC-988711 for **1** and **2**, respectively (Fax: +44 1223 336 033; E-mail: deposit@ccdc.cam.ac.uk; http://www.ccdc.cam.ac.uk).

References

[1] N. Fischer, T.M. Klapötke, M. Reymann, J. Stierstorfer. *Eur. J. Inorg. Chem.*, **12**, 2167 (2013).
[2] Y. Cui, T.L. Zhang, J.G. Zhang, X.C. Hu, J. Zhang, H.S. Huang. *Chin. J. Chem.*, **26**, 426 (2008).
[3] J.C. Gálvez-Ruiz, G. Holl, K. Karaghiosoff, T.M. Klapötke, K. Löhnwitz, P. Mayer, H. Nöth, K. Polborn, C.J. Rohbogner, M. Suter, J.J. Weigand. *Inorg. Chem.*, **44**, 4237 (2005).
[4] B. Gutmann, T.N. Glasnov, T. Razzaq, W. Goessler, D.M. Roberge, C.O. Kappe. *Beilstein J. Org. Chem.*, **7**, 503 (2011).
[5] S.N. Semenov, A.Y. Rogachev, S.V. Eliseeva, Y.A. Belousov, A.A. Drozdov, S.I. Troyanov. *Polyhedron*, **26**, 4899 (2007).
[6] G.H. Tao, B. Twamley, J.N.M. Shreeve. *Inorg. Chem.*, **48**, 9918 (2009).
[7] Q.G. Zhai, S.N. Li, X. Gao, W.J. Ji, Y.C. Jiang, M.C. Hu. *Inorg. Chem. Commun.*, **13**, 211 (2010).
[8] X.M. Zhang, Y.F. Zhao, H.S. Wu, S.R. Batten, S.W. Ng. *Dalton Trans.*, **26**, 3170 (2006).
[9] M. Friedrich, J.C. Gálvez-Ruiz, T.M. Klapötke, P. Mayer, B. Weber, J.J. Weigand. *Inorg. Chem.*, **44**, 8044 (2005).
[10] A.S. Lyakhov, P.N. Gaponik, S.V. Voitekhovich. *Acta Cryst.*, **57**, 185 (2001).
[11] V.E. Matulis, A.S. Lyakhov, P.N. Gaponik, S.V. Voitekhovich. *J. Mol. Struct.*, **649**, 309 (2003).
[12] X.B. Zhang, Y.H. Ren, W. Li, F.Q. Zhao, J.H. Yi, B.Z. Wang, J.R. Song. *J. Coord. Chem.*, **66**, 2051 (2013).
[13] Y. Tang, H. Yang, B. Wu, X. Ju, C. Lu, G. Cheng. *Angew. Chem. Int. Ed.*, **52**, 4875 (2013).
[14] S.V. Voitekhovich, P.N. Gaponik, A.S. Lyakhov, O.A. Ivashkevich. *Tetrahedron*, **64**, 872 (2008).
[15] P.N. Gaponik, M.M. Degtyarik, A.S. Lyakhov, V.E. Matulis, O.A. Ivashkevich, M. Quesada, J. Reedijk. *Inorg. Chim. Acta*, **358**, 3949 (2005).
[16] P.N. Gaponik, S.V. Voitekhovich, A.S. Lyakhov, V.E. Matulis, O.A. Ivashkevich, M. Quesada, J. Reedijk. *Inorg. Chim. Acta*, **358**, 2549 (2005).
[17] F. Li, X. Cong, Z. Du, C. He, L. Zhao, L. Meng. *New J. Chem.*, **36**, 1953 (2012).

[18] L. Liu, C. He, C. Li, Z. Li. *J. Chem. Crystallogr.*, **42**, 816 (2012).
[19] T.M. Klapötke. *Propellants Explos., Pyrotech.*, **35**, 213 (2010).
[20] T.M. Klapötke, F.A. Martin, J. Stierstorfer. *Chem. Eur. J.*, **18**, 1487 (2012).
[21] T.M. Klapötke, D.G. Piercey, J. Stierstorfer. *Eur. J. Inorg. Chem.*, **34**, 5694 (2012).
[22] T.M. Klapötke, C.M. Sabaté. *Eur. J. Inorg. Chem.*, **34**, 5350 (2008).
[23] Z.M. Li, J.G. Zhang, Y. Cui, T.L. Zhang, Y.J. Shu, V.P. Sinditskii, V.V. Serushkin, V.Y. Egorshin. *J. Chem. Eng. Data*, **55**, 3109 (2010).
[24] B. Tao, X. Jiang, X. Li, Y. Zhu, H. Xia. *J. Mol. Struct.*, **1001**, 111 (2011).
[25] Q.G. Zhai, S.N. Li, X. Gao, W.J. Ji, Y.C. Jiang, M.C. Hu. *Inorg. Chem. Commun.*, **13**, 211 (2010).
[26] B.D. Wu, T.L. Zhang, L. Yang, J.G. Zhang, Z.N. Zhou. *Z. Anorg. Allg. Chem.*, **639**, 163 (2013).
[27] Y. Cui, J.G. Zhang, T.L. Zhang, L. Yang, J. Zhang, X. Hu. *J. Hazard. Mater.*, **160**, 45 (2008).
[28] Y. Cui, J.G. Zhang, T.L. Zhang, L. Yang, Y. Zang, Y.J. Shu. *Chin. J. Chem.*, **26**, 2029 (2008).
[29] Y. Cui, T.L. Zhang, J.G. Zhang, L. Yang, J. Zhang, X. Hu. *Propellants., Explos Pyrotech.*, **33**, 437 (2008).
[30] G.M. Sheldrick. *SHELXS-97, Program for the Solution of Crystal Structures*, University of Göttingen, Germany (1997).
[31] (a) G.M. Sheldrick. *SHELXS-97, Program for the Refinement of Crystal Structures*, University of Göttingen, Germany (1997); (b) V. Dolomanov, L.J. Bourhis, R.J. Gildea, J.A.K. Howard, H.J. Puschmann. *Appl. Cryst.*, **42**, 339 (2009).
[32] Y.X. Ou. Explosives, p. 143, Beijing Institute of Technology Press, Beijing, China (2006).
[33] H.E. Kissinger. *Anal. Chem.*, **29**, 1702 (1957).
[34] T. Ozawa. *Chem. Soc. Jpn.*, **38**, 1881 (1965).
[35] T.L. Zhang, R.Z. Hu, Y. Xie, F.P. Li. *Thermochim. Acta*, **244**, 171 (1994).
[36] Z.M. Li, T.L. Zhang, G.T. Zhang, Z.N. Zhou, L. Yang, J.G. Zhang, K.B. Yu. *J. Coord. Chem.*, **66**, 1276 (2013).
[37] Q. Yang, S. Chen, G. Xie, S. Gao. *J. Coord. Chem.*, **65**, 2584 (2012).
[38] B.D. Wu, Y.G. Bi, Z.N. Zhou, L. Yang, J.G. Zhang, T.L. Zhang. *J. Coord. Chem.*, **66**, 3014 (2013).
[39] Z. Gao, J. Huang, K.Z. Xu, W.T. Zhang, J.R. Song, F.Q. Zhao. *J. Coord. Chem.*, **66**, 3572 (2013).